RESEARCH ARTICLE

Check for updates

Rotation of fullerene molecules in the crystal lattice of fullerene/porphyrin: C_{60} and $Sc_3N@C_{80}$†

Yajuan Hao,‡[a,b] Yaofeng Wang,‡[a] Lukas Spree [ID] [a] and Fupin Liu [ID] *[a]

The dynamics of molecules in the solid-state is important to understand their physicochemical properties. The temperature-dependent dynamics of $Sc_3N@C_{80}$ and C_{60} in the crystal lattice containing nickel octa-ethylporphyrin (NiOEP) was studied with variable temperature X-ray diffraction (VT-XRD). The results indicate that the fullerene cages (both C_{60} and C_{80}) in the crystal lattice present stronger libration than the co-crystallized NiOEP in the temperature range of 100−280 K. In contrast to the fullerene cage, the Sc_3N cluster shows pronounced rotation roughly perpendicular to the plane of the co-crystallized NiOEP molecule driven by temperature. The obtained temperature dependent dynamic behavior of the Sc_3N cluster is different from that of Ho_2LuN and Lu_3N, regardless of their rather similar structure, indicating the effect of the mass and size of the metal ions.

The empty inner space of fullerenes offers the possibility to use them as nano-containers to store atoms/clusters, leading to compounds known as endohedral fullerenes.[1] The encapsulation of trimetallic nitride clusters is well known and the resulting nitride clusterfullerenes show great potential in biomedicine and molecular magnetism.[2–8] The dynamics of fullerene molecules in the crystal lattice are fundamentally interesting. Recently, we unraveled the temperature driven molecular spinning top movement of Ho_2LuN/Lu_3N nitride clusters inside librating $I_h(7)$-C_{80} fullerene cages (hereafter the symmetry notation $I_h(7)$ will be omitted for clarity) and circular movement of Dy_2 inside benzyl functionalized C_{80}.[9–11] The fullerene/metal octaethylporphyrin (MOEP) co-crystallization method is widely applied to elucidate fullerene structures. However, the temperature dependent fullerene dynamics are rarely touched, considering the large number of such co-crystals reported. This is likely owing to the challenges presented by the need for high-quality crystals and technical effort required to undertake variable temperature X-ray diffraction measurements (VT-XRD). Phase transitions in crystals containing fullerenes were observed for several cases, such as, $Li@C_{60}$/NiOEP,[12] C_{60}/S_8,[13] C_{60}/CS_2,[14] C_{60}/C_6H_6,[15] C_{60}/C_2Cl_4.[16] C_{60}/CoOEP was reported more than two decades ago.[17]

Recently, the effect of the metal ion in the porphyrin and the role of the solvent in the crystallization of C_{60}/MOEP (M = Co, Ni, Cu, and Zn) was thoroughly investigated.[18,19] However, the temperature driven fullerene molecule dynamics in the crystal lattice of co-crystals with MOEP are still unclear for this type of fullerene. The structure of the nitride clusterfullerene $Sc_3N@C_{80}$ was reported more than two decades ago.[2] Later on, several efforts to elucidate the ordered crystal structure of $Sc_3N@C_{80}$ based on other co-crystallization routes were reported, a reasonably ordered structure was achieved with *o*-xylene,[20] disordered structures were obtained with cyclic Zn bis-porphyrin,[21] and $Sc_3N@C_{80}$ anions with counterions,[22,23] meanwhile, structures with well-ordered fullerene cages and disordered Sc_3N clusters have been observed with *o*-dichlorobenzene,[22] and decapyrrylcorannulene.[24] In strong contrast with the enthusiasm to get an ordered $Sc_3N@C_{80}$ structure with alternative co-crystallization strategies, the temperature dependent dynamics of $Sc_3N@C_{80}$ in the crystal lattice was never touched. Herein, we report on the temperature dependent dynamics of $Sc_3N@C_{80}$ in the crystal lattice, revealing the metallic atom effect on the dynamics of $M_3N@C_{80}$. Additionally, as a comparison, dynamics of C_{60} in a co-crystal of fullerene/NiOEP were unraveled to shed light on the understanding of the temperature dependent dynamics of fullerene/NiOEP crystals.

High-quality single crystals were obtained by co-crystallization of fullerenes (obtained by DC arc discharge synthesis as described previously[25]) with NiOEP.[17] X-ray diffraction data collection was carried out at the MX14.2 beamline of the BESSY storage ring (Berlin-Adlershof, Germany).[26] XDSAPP2.0 suite was employed for data processing.[27,28] The structure was solved by direct methods and refined by SHELXL-2018.[29] Hydrogen atoms were added geometrically, and refined with a

[a] *Leibniz Institute for Solid State and Materials Research (IFW Dresden), Helmholtzstraße 20, 01069 Dresden, Germany. E-mail: f.liu@ifw-dresden.de*
[b] *School of Electrical and Mechanical Engineering, Pingdingshan University, 467000 Pingdingshan, China*

‡These authors contributed equally to this work.

122 | *Inorg. Chem. Front.*, 2021, **8**, 122–126

This journal is © the Partner Organisations 2021

riding model. The crystal data are presented in Tables S1 and S2 in the ESI.† Fig. 1 shows the structures measured at variable temperatures from 100 to 280 K, the structures are shown from one specific direction to intuitively compare the temperature effect. The C_{60} molecule is nestled by four ethyl groups of the NiOEP, while the $Sc_3N@C_{80}$ molecule is embraced by all eight ethyl groups, which is archetypical for fullerene/NiOEP co-crystals. Overall, the temperature changing from 100 to 280 K does not enable rotation while the libration of the fullerene cage increased with the temperature as shown by the increasing size of the thermal ellipsoids as shown in Fig. 1 and 2. However, when comparing the increasing size of the thermal ellipsoids between fullerene molecule and the co-crystallized NiOEP, it does show that the fullerene cage librates stronger than its companion NiOEP. The temperature dependent dynamic behaviours of C_{60} and C_{80} in the crystal lattice are not significantly different in spite of the different relationships to the co-crystallized NiOEP molecule. The thermal ellipsoids of fullerene cage carbons are characteristic with small radial increments along with large lateral increments with temperature (shown in the highlighted part of Fig. 1 and Fig. S1†), indicating the increasing librational amplitudes experienced by the fullerene cages. The rather isotropic feature of the lateral ellipsoids is a sign of the isotropic libration of fullerene cages on the NiOEP. At 100 K, the shortest cage carbon to Ni distances are 2.766(3) Å and 3.006(2) Å for $Sc_3N@C_{80}$ and C_{60},

respectively. More details on higher temperatures are presented in Table S3 in the ESI.† The large difference between the cage carbon to Ni distance mirrors the rather different relationships between C_{60} or C_{80} and the NiOEP. C_{60} prefers to interact with half of the NiOEP molecule while $Sc_3N@C_{80}$ prefers the whole NiOEP, the plausible reason is the different size of the C_{60} and C_{80} in spite of the same icosahedral symmetry. The structure of $Sc_3N@C_{80}$ is consistent with the reported structures from co-crystals of pristine $Sc_3N@C_{80}$ as shown in Fig. S2–S10 in the ESI.†

Fig. 3 presents the distribution of the Sc_3N cluster at variable temperatures from 100 to 280 K with comparison of the analogous Ho_2LuN cluster, comparison between all measured temperatures is shown in Fig. S11.† The size of the metal ions represents the site occupancies, which are presented in detail in Table S4 in the ESI.† The N atom presents as ordered in the whole temperature ranging from 100 to 280 K, while the Sc atoms show increasing number of sites with increasing temperature, a sign of increasing movement at higher temperature. This is similar to the case of recently reported $M_3N@C_{80}$ (M_3 = Ho_2Lu, Lu_3),[9] because the encapsulated M_3N cluster rotates with the N as rotation center. However, there is a clear difference when comparing the $Sc_3N@C_{80}$ to its analogue $Ho_2LuN@C_{80}$. Ho_2LuN shows temperature dependent dynamics of mimicking the motion of spinning top, while the Sc_3N shows roughly free rotation on the plane nearly perpen-
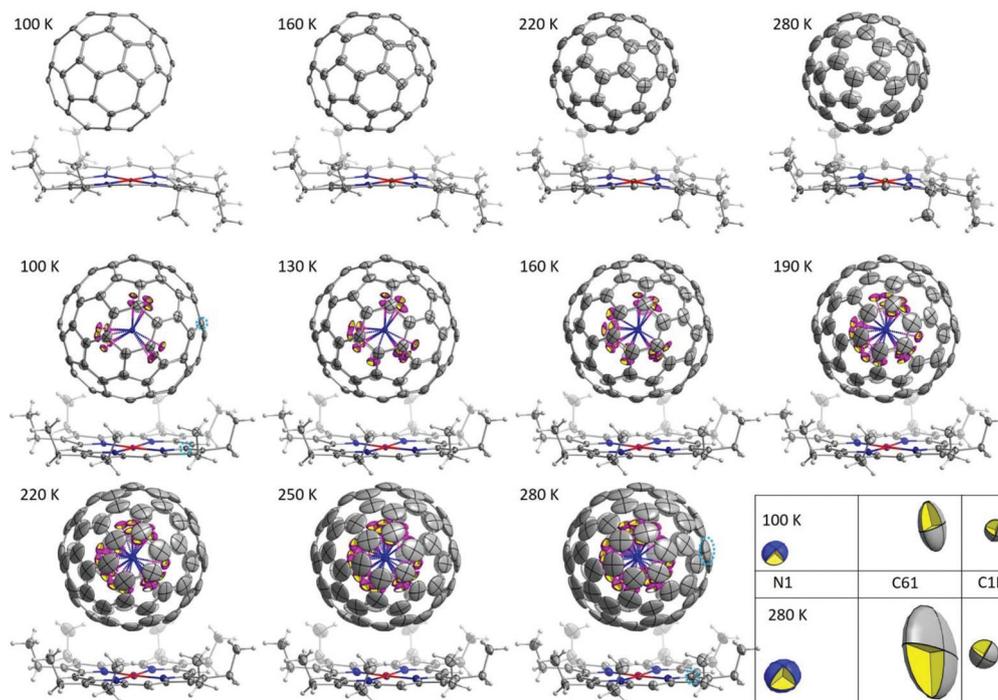

Fig. 1 Molecular structures of C_{60}/NiOEP and $Sc_3N@C_{80}$/NiOEP measured at variable temperatures. The solvent molecules are omitted for clarity. The displacement parameters are shown at the 30% probability level. Color code: grey for carbon, blue for nitrogen, white for hydrogen, red for nickel, and pink for scandium. To compare the ellipsoid changes upon temperature between cage carbon and NiOEP carbon, ellipsoids of C1P of NiOEP and C61 of C_{80} fullerene cage (both atoms are highlighted with a light blue circle in the related structures) at 100 and 280 K are highlighted at 80% probability level, the N1 of the Sc_3N cluster is drawn to show the orientation of the C61 as well as its ellipsoid changes on temperature.
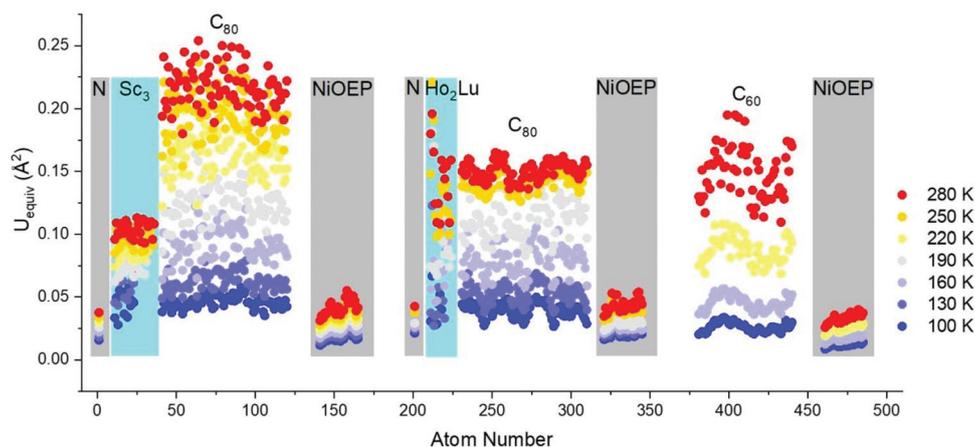
This journal is © the Partner Organisations 2021

Inorg. Chem. Front., 2021, **8**, 122–126 | **123**

Fig. 2 Comparison of equivalent atomic displacement parameters of $Sc_3N@C_{80}\cdot NiOEP\cdot 2(C_6H_6)$, $C_{60}/NiOEP/C_7H_8/C_6H_6$ and $Ho_2LuN@C_{80}\cdot NiOEP\cdot 2(C_6H_6)^9$ as a function of temperature between 100 and 280 K. The encapsulated N and co-crystallized NiOEP were highlighted with grey rectangles, while the encapsulated metals were highlighted with cyan rectangles.
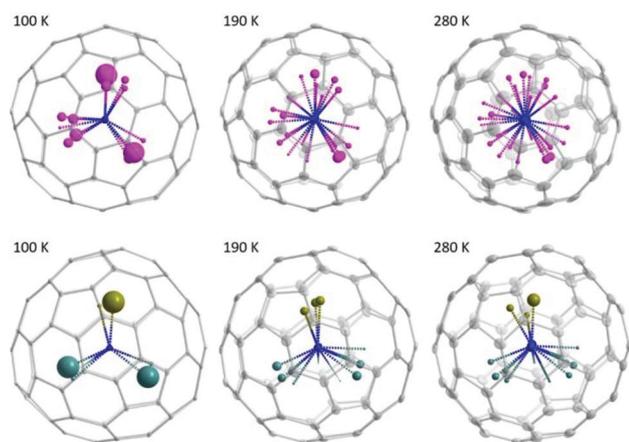

Fig. 3 Molecular structure of $Sc_3N@C_{80}\cdot NiOEP\cdot 2(C_6H_6)$ measured with single-crystal X-ray diffraction at variable temperatures from 100 to 280 K. The metal sites are shown as spheres whose radii are scaling proportional to the site occupancy (the bigger the sphere, the higher the occupancy). Color code: grey for carbon, pink for Sc, and blue for N. As comparison, the molecular structure of $Ho_2LuN@C_{80}\cdot NiOEP\cdot 2(C_6H_6)$ measured with single-crystal X-ray diffraction at variable temperatures from 100 to 280 K was shown.[9] The metal sites are shown as spheres whose radii are scaling proportional to the site occupancy (the bigger the sphere, the higher the occupancy). Color code: grey for carbon, brown for Lu, cyan for Ho, and blue for N.

dicular to the NiOEP plane. This is further shown in Fig. 4 with the observed electron density maps at 100 and 280 K. This is significant, because considering the very similar structure of $Ho_2LuN@C_{80}$ and $Sc_3N@C_{80}$ from the perspectives of fullerene cage (the same), the M_3N cluster (both planar cluster with similar M–N bond lengths and M–N–M bond angles), and the M-cage carbon distances, the temperature dependent dynamics would be expected to be similar. However, it is different. The plausible explanation is that the mass and size of the M^{3+} ions matter. When the encapsulated cluster is Ho_2LuN or Lu_3N, the temperature dependent dynamics of the cluster are the same because the mass and size differences between Ho(M = 165 g mol^{-1}, r^{3+} = 0.901 Å (ref. 30)) and Lu(M = 175 g mol^{-1}, r^{3+} = 0.861 Å (ref. 30)) are not significant when comparing them to the much lighter Sc(M = 45 g mol^{-1}, r^{3+} = 0.745 Å (ref. 30)). It is worth to mention that Balch *et al.* highlighted the interesting phenomenon in $M_3N@C_{80}$ cocrystals with NiOEP, which shows a strong tendency for M_3N to be situated over one of the N–Ni–N set of bonds within the NiOEP.[31,32] The temperature driven rotation of Sc_3N and Ho_2LuN clusters in C_{80} cage relative to the co-crystallized NiOEP viewed from the direction perpendicular to porphyrin plane are presented in Fig. S12.†
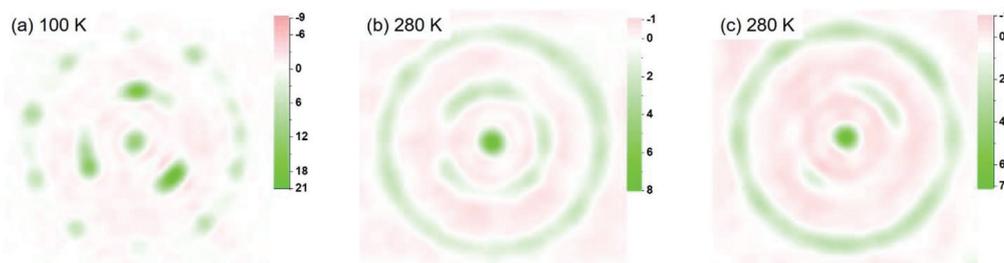

Fig. 4 Observed electron density maps of the Sc_3N cluster. (a) Plane map passing through the encapsulated Sc_3N (main site composed of Sc2, Sc3, and Sc9) at 100 K. (b) Plane map roughly perpendicular to the NiOEP plane passing through the encapsulated Sc_3N (relatively main site composed of Sc2, Sc9, and Sc12) at 280 K. (c) Plane map roughly parallel to the NiOEP plane passing through the encapsulated N atom at 280 K.

Conclusion

The temperature-dependent dynamics of $Sc_3N@C_{80}$ and C_{60} in the crystal lattice containing the widely used co-crystallization reagent, nickel octaethylporphyrin (NiOEP), was studied with variable temperature X-ray diffraction. The results indicate that the rotation of fullerene cages (both C_{60} and C_{80}) in the crystal lattice is suppressed in the temperature range of 100–280 K, while libration of the fullerene cages comparing with the co-crystallized NiOEP is clearly promoted with increasing temperature. The most striking result is that the temperature dependent dynamic behavior of the encapsulated Sc_3N cluster is different from that of its analogues, Ho_2LuN/Lu_3N, regardless of the rather similar structure, which can be explained by the difference in mass and size of the M^{3+} ions. The results shed light on how the dynamics of the widely surveyed $M_3N@C_{80}$ system are influenced by metal ion mass and size.

Conflicts of interest

There are no conflicts to declare.

Acknowledgements

References

1 A. A. Popov, S. Yang and L. Dunsch, Endohedral Fullerenes, *Chem. Rev.*, 2013, **113**, 5989–6113.

2 S. Stevenson, G. Rice, T. Glass, K. Harich, F. Cromer, M. R. Jordan, J. Craft, E. Hadju, R. Bible, M. M. Olmstead, K. Maitra, A. J. Fisher, A. L. Balch and H. C. Dorn, Small-bandgap endohedral metallofullerenes in high yield and purity, *Nature*, 1999, **401**, 55–57.

3 J. Zhang, S. Stevenson and H. C. Dorn, Trimetallic Nitride Template Endohedral Metallofullerenes: Discovery, Structural Characterization, Reactivity, and Applications, *Acc. Chem. Res.*, 2013, **46**, 1548–1557.

4 T. Wang and C. Wang, Functional Metallofullerene Materials and Their Applications in Nanomedicine, Magnetics, and Electronics, *Small*, 2019, **15**, e1901522.

5 F. Liu, L. Spree, D. S. Krylov, G. Velkos, S. M. Avdoshenko and A. A. Popov, Single-Electron Lanthanide-Lanthanide Bonds Inside Fullerenes toward Robust Redox-Active Molecular Magnets, *Acc. Chem. Res.*, 2019, **52**, 2981–2993.

6 L. Spree and A. A. Popov, Recent advances in single molecule magnetism of dysprosium-metallofullerenes, *Dalton Trans.*, 2019, **48**, 2861–2871.

7 S. Yang, T. Wei and F. Jin, When metal clusters meet carbon cages: endohedral clusterfullerenes, *Chem. Soc. Rev.*, 2017, **46**, 5005–5058.

8 T. Li and H. C. Dorn, Biomedical Applications of Metal-Encapsulated Fullerene Nanoparticles, *Small*, 2017, **13**, 1603152.

9 F. Liu and L. Spree, Molecular Spinning Top: Visualizing the Dynamics of $M_3N@C_{80}$ with Variable Temperature Single Crystal X-ray Diffraction, *Chem. Commun.*, 2019, **55**, 13000–13003.

10 F. Liu, G. Velkos, D. S. Krylov, L. Spree, M. Zalibera, R. Ray, N. A. Samoylova, C.-H. Chen, M. Rosenkranz, S. Schiemenz, F. Ziegs, K. Nenkov, A. Kostanyan, T. Greber, A. U. B. Wolter, M. Richter, B. Büchner, S. M. Avdoshenko and A. A. Popov, Air-stable redox-active nanomagnets with lanthanide spins radical-bridged by a metal–metal bond, *Nat. Commun.*, 2019, **10**, 571.

11 F. Liu, D. S. Krylov, L. Spree, S. M. Avdoshenko, N. A. Samoylova, M. Rosenkranz, A. Kostanyan, T. Greber, A. U. B. Wolter, B. Büchner and A. A. Popov, Single molecule magnet with an unpaired electron trapped between two lanthanide ions inside a fullerene, *Nat. Commun.*, 2017, **8**, 16098.

12 H. Ueno, S. Aoyagi, Y. Yamazaki, K. Ohkubo, N. Ikuma, H. Okada, T. Kato, Y. Matsuo, S. Fukuzumi and K. Kokubo, Electrochemical Reduction of Cationic $Li^+@C_{60}$ to Neutral $Li^+@C_{60}^{\bullet-}$: Isolation and Characterisation of Endohedral [60]Fulleride, *Chem. Sci.*, 2016, **7**, 5770–5774.

13 K. B. Ghiassi, S. Y. Chen, J. Wescott, A. L. Balch and M. M. Olmstead, New Insights into the Structural Complexity of $C_{60}\cdot2S_8$: Two Crystal Morphologies, Two Phase Changes, Four Polymorphs, *Cryst. Growth Des.*, 2015, **15**, 404–410.

14 M. M. Olmstead, F. Jiang and A. L. Balch, $2C_{60}\cdot3CS_2$: orientational ordering accompanies the reversible phase transition at 168 K, *Chem. Commun.*, 2000, 483–484, DOI: 10.1039/a908147j.

15 M. M. Olmstead, A. L. Balch and H. M. Lee, An order–disorder phase transition in the structure of $C_{60}\cdot4$benzene, *Acta Crystallogr., Sect. B: Struct. Sci.*, 2012, **68**, 66–70.

16 C. J. Chancellor, F. L. Bowles, J. U. Franco, D. M. Pham, M. Rivera, E. A. Sarina, K. B. Ghiassi, A. L. Balch and M. M. Olmstead, Single-Crystal X-ray Diffraction Studies of Solvated Crystals of C_{60} Reveal the Intermolecular Interactions between the Component Molecules, *J. Phys. Chem. A*, 2018, **122**, 9626–9636.

17 M. M. Olmstead, D. A. Costa, K. Maitra, B. C. Noll, S. L. Phillips, P. M. Van Calcar and A. L. Balch, Interaction of curved and flat molecular surfaces. The structures of crystalline compounds composed of fullerene (C_{60}, $C_{60}O$, C_{70}, and $C_{120}O$) and metal octaethylporphyrin units, *J. Am. Chem. Soc.*, 1999, **121**, 7090–7097.

18 M. Roy, M. M. Olmstead and A. L. Balch, Metal Ion Effects on Fullerene/Porphyrin Cocrystallization, *Cryst. Growth Des.*, 2019, **19**, 6743–6751.

This journal is © the Partner Organisations 2021

Inorg. Chem. Front., 2021, **8**, 122–126 | **125**

19 M. Roy, I. D. Diaz Morillo, X. B. Carroll, M. M. Olmstead and A. L. Balch, Solvent and Solvate Effects on the Cocrystallization of C_{60} with Co^{II}(OEP) or Zn^{II}(OEP) (OEP = Octaethylporphyrin), *Cryst. Growth Des.*, 2020, **20**, 5596–5609.

20 S. Stevenson, H. M. Lee, M. M. Olmstead, C. Kozikowski, P. Stevenson and A. L. Balch, Preparation and crystallographic characterization of a new endohedral, $Lu_3N@C_{80}\cdot5$ (*o*-xylene), and comparison with $Sc_3N@C_{80}\cdot5$ (*o*-xylene), *Chem. – Eur. J.*, 2002, **8**, 4528–4535.

21 L. P. Hernández-Eguía, E. C. Escudero-Adán, J. R. Pinzón, L. Echegoyen and P. Ballester, Complexation of $Sc_3N@C_{80}$ Endohedral Fullerene with Cyclic Zn-Bisporphyrins: Solid State and Solution Studies, *J. Org. Chem.*, 2011, **76**, 3258–3265.

22 D. Konarev, A. A. Popov, L. V. Zorina, S. S. K. Khasanov and R. N. Lyubovskaya, Molecular structure, magnetic and optical properties of endometallonitridofullerene $Sc_3N@I_h,-C_{80}$ in neutral, radical anion and dimeric anionic forms, *Chem. – Eur. J.*, 2019, **25**, 14858–14869.

23 D. V. Konarev, L. Zorina, S. S. Khasanov, A. A. Popov, A. Otsuka, H. Yamochi, G. Saito and R. N. Lyubovskaya, Crystalline anionic complex of scandium nitride endometallo-fullerene: Experimental observation of single-bonded $(Sc_3N@I_h,-C_{80}^-)_2$ dimers, *Chem. Commun.*, 2016, **52**, 10763–10766.

24 Y.-Y. Xu, H.-R. Tian, S.-H. Li, Z.-C. Chen, Y.-R. Yao, S.-S. Wang, X. Zhang, Z.-Z. Zhu, S.-L. Deng, Q. Zhang, S. Yang, S.-Y. Xie, R.-B. Huang and L.-S. Zheng, Flexible decapyrrylcorannulene hosts, *Nat. Commun.*, 2019, **10**, 485.

25 D. S. Krylov, F. Liu, S. M. Avdoshenko, L. Spree, B. Weise, A. Waske, A. U. B. Wolter, B. Büchner and A. A. Popov, Record-high thermal barrier of the relaxation of magnetiza-

tion in the nitride clusterfullerene $Dy_2ScN@C_{80}-I_h$, *Chem. Commun.*, 2017, **53**, 7901–7904.

26 U. Mueller, R. Förster, M. Hellmig, F. U. Huschmann, A. Kastner, P. Malecki, S. Pühringer, M. Röwer, K. Sparta, M. Steffien, M. Ühlein, P. Wilk and M. S. Weiss, The macromolecular crystallography beamlines at BESSY II of the Helmholtz-Zentrum Berlin: Current status and perspectives, *Eur. Phys. J. Plus*, 2015, **130**, 141.

27 K. M. Sparta, M. Krug, U. Heinemann, U. Mueller and M. S. Weiss, XDSAPP2.0, *J. Appl. Crystallogr.*, 2016, **49**, 1085–1092.

28 W. Kabsch, XDS, *Acta Crystallogr., Sect. D: Biol. Crystallogr.*, 2010, **66**, 125–132.

29 G. Sheldrick, Crystal structure refinement with SHELXL, *Acta Crystallogr., Sect. C: Cryst. Struct. Commun.*, 2015, **71**, 3–8.

30 R. Shannon, Revised effective ionic radii and systematic studies of interatomic distances in halides and chalcogenides, *Acta Crystallogr., Sect. A: Cryst. Phys., Diffr., Theor. Gen. Crystallogr.*, 1976, **32**, 751–767.

31 S. Stevenson, C. J. Chancellor, H. M. Lee, M. M. Olmstead and A. L. Balch, Internal and external factors in the structural organization in cocrystals of the mixed-metal endohedrals $(GdSc_2N@I_h,-C_{80}, Gd_2ScN@I_h,-C_{80},$ and $TbSc_2N@I_h,-C_{80})$ and nickel(II) octaethylporphyrin, *Inorg. Chem.*, 2008, **47**, 1420–1427.

32 M. M. Olmstead, T. Zuo, H. C. Dorn, T. Li and A. L. Balch, Metal Ion Size and the Pyramidalization of Trimetallic Nitride Units Inside a Fullerene Cage: Comparisons of the Crystal Structures of $M_3N@I_h,-C_{80}$ (M = Gd, Tb, Dy, Ho, Er, Tm, Lu, and Sc) and Some Mixed Metal Counterparts, *Inorg. Chim. Acta*, 2017, **468**, 321–326.